

## Effect of Two-neutron Transfer with Positive $Q$ -value on Sub-barrier Fusion

C. J. Lin<sup>a</sup>, H. M. Jia, H. Q. Zhang, X. X. Xu, F. Yang, L. Yang, P. F. Bao, L. J. Sun, and Z. H. Liu

China Institute of Atomic Energy, P. O. Box 275(10), Beijing 102413, China

**Abstract.** Fusion cross sections with high precision have been measured for the  $^{16}\text{O}+^{76}\text{Ge}$  and  $^{18}\text{O}+^{74}\text{Ge}$  systems at energies near and below the Coulomb barrier. Coupled-channels calculations including inelastic excitations well reproduce the experimental fusion excitation functions and the corresponding barrier distributions. There is no evidence that the positive  $Q$ -value two-neutron transfer plays a role in the fusion process. Systematic investigations of  $^{18}\text{O}$  induced fusions, whose data are available in the literature, have been performed to understand the role of two-neutron transfers with positive  $Q$ -values in the fusion process, but results are inconsistent and no conclusion can be made. The effect of two-neutron transfer with positive  $Q$ -value on sub-barrier fusion is still an open question, which becomes a challenge and requires further efforts both experimentally and theoretically.

### 1 Introduction

The coupled-channels (CC) effect plays a crucial role in heavy-ion fusion process at near- and sub-barrier energy region. Couplings between the intrinsic degrees of freedom of the reactants and the degree of freedom of relative motion result in enhancement of fusion cross sections, broadening of spin distributions of compound nuclei, single barrier splitting into a distribution, and so on. Coupling of transfer reaction to fusion is a complex procedure, which requires ones to comprehensively understand the mechanisms of transfer and fusion. For neutron transfer, because neutron is a neutral particle, reaction may take place at a large distance and form a neutron flow, resulting in fusion enhancement. Further, for neutron transfer with positive  $Q$ -value, the kinetic energy of reaction system may increase, leading to fusion enhancement too. For the above reasons, the effect of positive  $Q$ -value neutron transfer (PQNT) on fusion, especially at sub-barrier energies, becomes an important topic of current interest.

The idea of PQNT effect stems from an experimental observation. In 1980, Beckerman *et al.* [1] measured the fusion excitation functions of  $^{58}\text{Ni}+^{58}\text{Ni}$ ,  $^{58}\text{Ni}+^{64}\text{Ni}$ , and  $^{64}\text{Ni}+^{64}\text{Ni}$ , and found that the fusion of  $^{58}\text{Ni}+^{64}\text{Ni}$  is strongly enhanced compared to other two systems. Three year later, R. A. Broglia *et al.* [2] proposed that two neutrons transfer should be responsible for this enhancement. In their explanation, fusion will be favoured in a transfer channel if  $Q+\Delta E^{\text{C}} > 0$ , where  $\Delta E^{\text{C}}$  is the difference of the Coulomb barrier heights between the incoming channel and the outgoing channel. Later, D.

Ackermann *et al.* [3] claimed that the direct two-neutron ( $2n$ ) transfer with  $Q = 3.9$  MeV, rather than the sequential neutron transfers, takes effect on the fusion enhancement of  $^{58}\text{Ni}+^{64}\text{Ni}$ . Following these pioneer works, systematic research for the reaction systems of  $^{28}\text{Si}+^{94}\text{Zr}$  [4],  $^{32}\text{S}+^{96}\text{Zr}$ ,  $^{100}\text{Mo}$ ,  $^{110}\text{Pd}$  [5-7], and  $^{40}\text{Ca}+^{48}\text{Ca}$ ,  $^{96}\text{Zr}$ ,  $^{124,132}\text{Sn}$  [8-12] has confirmed the fusion enhancement due to the PQNT channels by comparison with their reference systems. The role of multi-nucleon transfer channels has been extensively discussed in Ref. [13].

However, the relationship between fusion and neutron transfer is actually not clear yet. Theoretically, other mechanisms can also explain the experimental results without including the PQNT effects explicitly. For example, for the  $^{40}\text{Ca}+^{96}\text{Zr}$  system, both the enhancement of fusion cross sections and the shape of barrier distribution (BD) can be well reproduced by a semi-classical model, mainly considering the coupling of the strong  $3^-$  vibrational state of  $^{96}\text{Zr}$  [14]. Experimentally, there exist some negative observations. In the systems of  $^{18}\text{O}+^{92}\text{Mo}$ ,  $^{118}\text{Sn}$  [15,16],  $^{36}\text{S}+^{58}\text{Ni}$  [17], and  $^{58}\text{Ni}+^{100}\text{Mo}$ ,  $^{124}\text{Sn}$  [18–20], the fusion cross sections do not show additional enhancement at sub-barrier energies due to the PQNT channels. Recently, Kohley *et al.* [21] observed that fusion of the neutron-rich  $^{132}\text{Sn}+^{58}\text{Ni}$  system, with more PQNT channels, does not cause any enhancement in the fusion cross sections down to the  $\sim 5$  mb level by means of a systematic comparison to its reference system.

In order to further investigate the PQNT effect and to simplify the question, the  $^{16}\text{O}+^{76}\text{Ge}$  and  $^{18}\text{O}+^{74}\text{Ge}$  systems were selected, because: i) the same compound nucleus is formed for the two systems; ii) the

<sup>a</sup> Corresponding author: cjlin@ciae.ac.cn

corresponding excitation-energy levels and deformation parameters are quite similar for the two targets and the deformation effect of  $^{16,18}\text{O}$  is minor [22]; iii) the main difference in the two systems comes from the transfer reaction channel. The  $^{18}\text{O}+^{74}\text{Ge}$  system possesses a  $2n$  transfer channel with positive  $Q$ -value of 3.75 MeV, while the  $^{16}\text{O}+^{76}\text{Ge}$  system has no such reaction channel. The latter can be used as a reference system to explore the PQNT effect on the former, where the  $2n$  transfer is a simpler case which can be included in the CC calculations [23] as a pair transfer.

## 2 Experimental procedures

The experiment was performed at the HI-13 tandem accelerator of the China Institute of Atomic Energy (CIAE), Beijing, China. Collimated  $^{16,18}\text{O}$  ( $q = 5^+$ ) beams with an intensity of 20–30 pA were used to bombard the  $^{76,74}\text{Ge}$  targets. Beam energies were varied only downward in the range of 61–38 MeV in order to reduce the magnetic hysteresis. The  $^{74}\text{Ge}$  (99.7% enriched) and  $^{76}\text{Ge}$  (99.9% enriched) targets were  $120 \mu\text{g}/\text{cm}^2$  thick evaporated onto  $30 \mu\text{g}/\text{cm}^2$  carbon foil backing and  $50 \mu\text{g}/\text{cm}^2$  thick evaporated onto  $20 \mu\text{g}/\text{cm}^2$  carbon foil backing, respectively. Four silicon (Si) detectors, placed symmetrically at  $20^\circ$  (right-left and up-down) with respect to the beam direction, were used to monitor the Rutherford scattering and to provide a normalization of the fusion cross section.

Fusion evaporation residues (ERs) were separated from the beam-like particles (BLPs) by using an electrostatic deflector setup [24]. It consists of two pairs of electrodes followed by time-of-flight (TOF) versus  $E$  detector telescopes with two micro-channel plate (MCP) detectors and a  $48 \times 48 \text{ mm}^2$  quadrant Si detector. Figure 1 shows a typical TOF versus  $E$  spectrum for the  $^{18}\text{O}+^{74}\text{Ge}$  system at an energy around the Coulomb barrier, where the BLPs and ERs can be separated clearly. The particles from the target were selected before entering the electric fields by an entrance collimator of 2.5 mm in diameter, corresponding to an opening angle of  $0.76^\circ$ . A  $10 \mu\text{g}/\text{cm}^2$  thick carbon foil located at 19 cm downstream of the target was used to reset the atomic charge state distribution by an internal conversion process on the ion path. The ERs angular distributions were measured in the range from  $-5^\circ$  to  $13^\circ$  with a step of  $1^\circ$  for  $^{16}\text{O}+^{76}\text{Ge}$  at  $E_{\text{lab}} = 44.38 \text{ MeV}$  as well as  $^{18}\text{O}+^{74}\text{Ge}$  at  $E_{\text{lab}} = 45.40$  and  $40.39 \text{ MeV}$ , respectively. Their typical shapes do not change appreciably with the beam energy and give an overall width of  $4.3^\circ$  symmetrical about  $0^\circ$ . The ERs angular distributions were fitted by a single Gaussian function resulting from the dominant neutron evaporation from the CN, which is consistent with the calculation of the PACE2 [25] code. For most energies, the differential cross sections have been measured only at  $3^\circ$ . The fusion cross sections were obtained by integration of the angular distribution and normalized by the Rutherford scattering counted by the four Si monitors. Meanwhile, corrections were made for the solid angles and transmission efficiencies. Since fission of the CN can be neglected for

both systems, the measured ERs cross sections were regarded as complete fusion cross sections  $\sigma_{\text{Fus}}$ .

The transmission efficiencies and the relevant voltages used to deflect the ERs were calibrated with  $^{79}\text{Br}$  and  $^{127}\text{I}$  beams scattered by a  $^{208}\text{Pb}$  target at the corresponding energies to the ERs at  $13^\circ$ . It was found that the defocusing effect of the deflection voltage reduces the transmission to  $0.29 \pm 0.03$ . Altogether a systematic error of 15% is estimated considering additional systematic errors, which comes from the uncertainties of geometrical solid angle, the angular distribution integrations, and the transmission measurements.

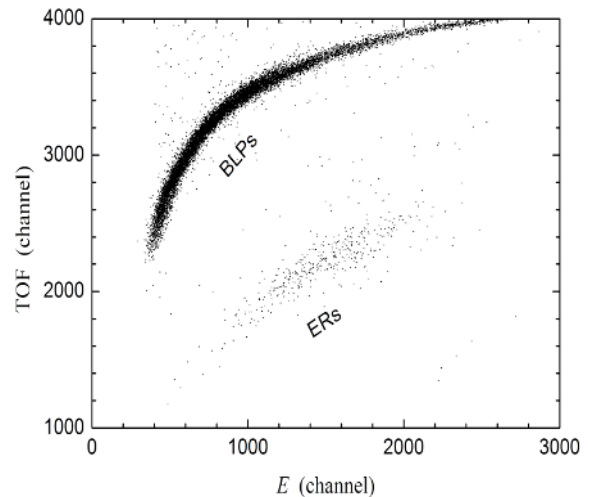


**Figure 1.** TOF-E matrix measured at the beam energy of 42.08 MeV to identify the BLPs and ERs.

## 3 Results and discussions

### 3.1 Results of $^{16}\text{O}+^{76}\text{Ge}$ and $^{18}\text{O}+^{74}\text{Ge}$

Fusion excitation functions for  $^{16}\text{O}+^{76}\text{Ge}$  and  $^{18}\text{O}+^{74}\text{Ge}$ , respectively, have been obtained with overall statistical uncertainties of about 1%. In order to understand the CC effects in the two fusion processes, the CCFULL [23] calculations with all order couplings have been performed by using the well-known Akyüz-Winther (AW) potential [26].

For comparison, the reduced fusion excitation functions are plotted in Fig.2 (top panel). For the  $^{16}\text{O}+^{76}\text{Ge}$  system, the low-lying vibrational  $2^+$  and  $3^-$  one-phonon states of the target, the same ones used in Ref. [27], as well as their mutual excitations were included in the calculations (see the dashed line in the figure). The higher excitation energy of the  $3^-$  one-phonon state of  $^{16}\text{O}$  only produces an adiabatic potential renormalization without affecting the structure in the BD [28], and, consequently, was not included in the CC calculations. For the  $^{18}\text{O}+^{74}\text{Ge}$  system, the lowest  $2^+$  two-phonon state as well as  $3^-$  one-phonon vibrational state of the target and the  $2^+$  state of  $^{18}\text{O}$  were included in the CC calculations (solid lines in Fig. 2). In order to check the effects of neutron transfer, the CC calculation was also performed by including the additional  $2n$ -pair transfer

channel with a positive  $Q$ -value of 3.75 MeV and the nominal coupling strength of 0.7 MeV (dash-dotted lines). The corresponding BDs are also illustrated in Fig. 2 (bottom panel). In the second derivative procedure for deducing BD, the energy step was taken as  $\sim 2$  MeV. Details of the analysis can be found in Ref. [29].

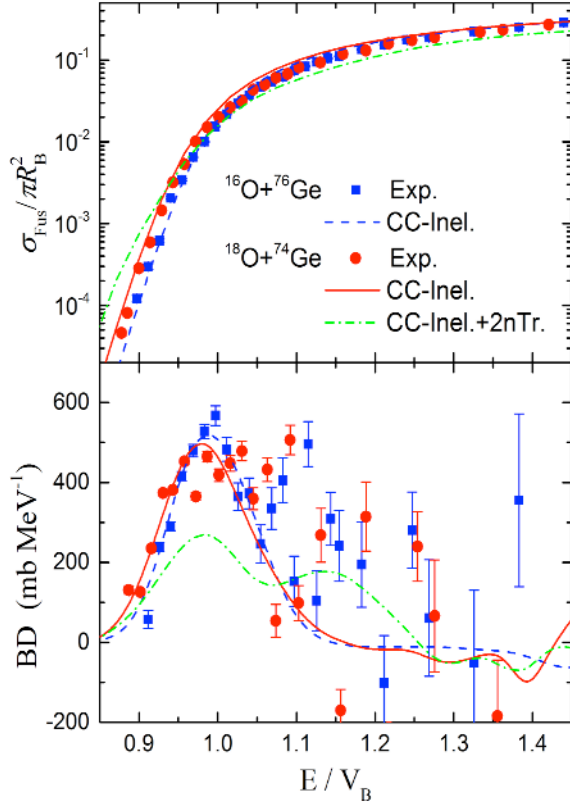


**Figure 2.** (Color online) Experimental reduced fusion excitation functions and barrier distributions compared with the coupled-channels calculations.

From Fig. 2, one can see that: i) both experimental fusion excitation functions and BDs are almost identical for the two systems. ii) CC calculations including the inelastic coupling (dashed and solid lines for  $^{16}\text{O}+^{76}\text{Ge}$  and  $^{18}\text{O}+^{74}\text{Ge}$ , respectively) are in good agreement with the experimental fusion excitation functions. For the BDs, CC calculations reproduce the main peaks at  $E/V_B \approx 1$  but fault at higher energies where the experimental BDs have large fluctuations due to the second derivative and the apparent second bumps at  $E/V_B \approx 1.2$  might be illusive. iii) CC calculations with an extra  $2n$ -pair transfer for the  $^{18}\text{O}+^{74}\text{Ge}$  system (dash-dotted lines) overestimate fusion cross sections below barrier but underestimate fusion cross sections above barrier and the calculated BD splits into two bumps, those are clearly inconsistent with experimental results. From the above analyses, one may conclude that there is no evidence showing the PQNT effect on the fusion process for the  $^{18}\text{O}+^{74}\text{Ge}$  system.

### 3.2 Systematics of $^{18}\text{O}$ induced fusions

For most of the  $^{18}\text{O}$  induced reactions, there exist  $2n$  transfer channels with positive  $Q$ -values. For this reason, it is worth doing a systematic investigation on  $^{18}\text{O}$

induced fusions whose data are available in literature to check the PQNT effect. Table 1 lists some typical systems of  $^{18}\text{O}$  induced fusions. Systems with targets heavier than Sn are not included here, because the fission barriers of compound nuclei become lower and the fission probabilities become larger at high energies. The fourth column of Tab.1 indicates whether the system possesses the PQNT effect compared to its reference system, i.e. the  $^{16}\text{O}$  induced fusion. Some of them are illustrated in Fig.3 for the sake of immediacy. From Tab. 1 and Fig. 3, one can see that: i) most of the systems have no PQNT effects except the  $^{18}\text{O}+^{58}\text{Ni}$  system; ii)  $^{18}\text{O}$  induced fusion data are available only at energies around and above the Coulomb barrier for most of the systems except the  $^{74}\text{Ge}$  and  $^{112-124}\text{Sn}$  targets.

**Table 1.** Some typical systems of  $^{18}\text{O}$  induced fusions.

Target	$Q_{1n}$	$Q_{2n}$	PQNT	Ref.
$^{24}\text{Mg}$	-0.71	6.24	N*	[30]
$^{27}\text{Al}$	-0.32	4.97	N*	[31,32]
$^{28}\text{Si}$	0.43	6.90	N*	[31]
$^{44}\text{Ca}$	-0.63	5.62	N*	[33]
$^{58}\text{Ni}$	0.96	8.20	Y*	[34,35]
$^{60,64}\text{Ni}$	-0.22/-1.95	6.23/2.86	N*	[35]
$^{63,65}\text{Cu}$	-0.13/-0.98	5.64/4.01	N*	[36]
$^{74}\text{Ge}$	-1.54	3.75	N	[29]
$^{92}\text{Mo}$	0.03	5.56	N*	[37]
$^{112-124}\text{Sn}$	< -0.30	> 1.74	N	[38]

\* Data available only around and above barrier

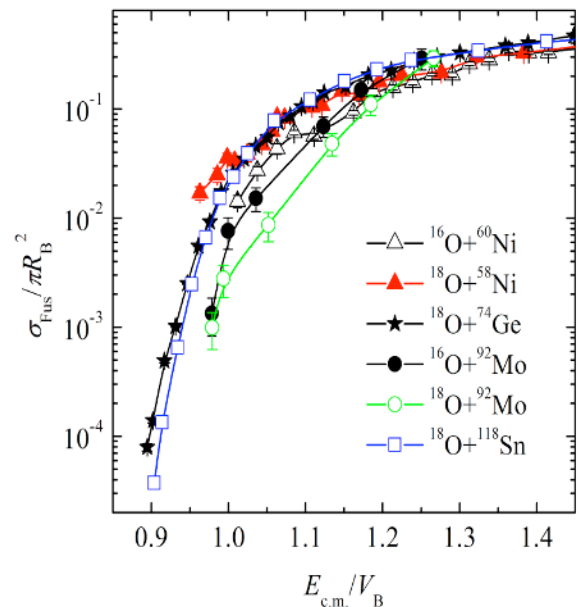


**Figure 3.** (Color online) Reduced fusion excitation functions for some typical systems.

For the  $^{18}\text{O}+^{58}\text{Ni}$  system, fusion enhancement undoubtedly exists although the cross sections were measured near the barrier [34,35], compared to its reference, the  $^{16}\text{O}+^{60}\text{Ni}$  system. Later the BD extracted from the backward quasi-elastic scattering [39] also supports this point. It is thought that the collective  $2n$ -pair transfer mode plays an important role. Such enhancement can be explained well by the zero-point pairing fluctuations model (pairing vibrations related to two-neutron transfer channel). However, the fusion behaviour of its neighbour systems, the  $^{18}\text{O}+^{60,64}\text{Ni}$  systems is markedly different, having no enhancement compared to the  $^{16}\text{O}$  reference systems.

### 3.3 Relation to transfer channels

For  $^{74}\text{Ge}(^{18}\text{O},^{16}\text{O})^{76}\text{Ge}$ , the experiment performed by Bond *et al.* [40] showed that the transfer mainly populates the ground state at  $27^\circ$  with a beam energy of 75 MeV. It denotes that the  $2n$  stripping channel is kinematically matched and neutron transfer should enhance the subsequent fusion at sub-barrier energies, as expected from ground-state to ground-state transfer at the sub-barrier region [41]. However, our results do not show such an effect by the comparison of the experimental data with CC calculations.

It is known that transfer couplings also depend on the states and  $Q$ -values populated by transferred nucleons and transfer form factors. For  $^{18}\text{O}$  induced reaction, the  $Q$ -value of  $2n$  stripping channel is usually positive. It is advantageous to use  $^{18}\text{O}$  as projectile to investigate the influence of the  $2n$  transfer channel on fusion. However, the relevant fusion data with high accuracy are rather scarce up to now. To measure the fusion excitation functions for these systems with high accuracy may help us to clarify the relevant dynamic mechanisms. On the other hand, direct measurements of the  $2n$  transfers are also meaningful for correlating the two aspects of fusion and transfer and constraining the transfer coupling strengths.

## 4 Summary

In summary, fusion cross sections have been measured for the  $^{16}\text{O}+^{76}\text{Ge}$  and  $^{18}\text{O}+^{74}\text{Ge}$  systems at energies near and below the barrier. The BDs were extracted from the second derivative of the excitation functions. The fusion behaviour of the two systems shows remarkable similarities and can be reproduced well by the CC calculations with the low-lying inelastic states being taken into account for the two systems. This is beyond the expectation for  $^{18}\text{O}+^{74}\text{Ge}$  in the case of a positive  $Q_{-2n}$  neutron transfer channel.

The effect of neutron transfer on fusion is still an open question. The controversial PQNT effect on fusion observed in the fusion reactions has presented a challenge for the theoretical understanding of the reaction mechanism. It is highly desired to search for the origin responsible for these inconsistencies of fusion in correlation with PQNT channels and to improve the CC theory or other models.

## References

1. M. Beckerman *et al.*, Phys. Rev. Lett. **45**, 1472 (1980).
2. R. A. Broglia *et al.*, Phys. Rev. C **27**, 2433 (1983).
3. D. Ackermann *et al.*, Nucl. Phys. **A583**, 129 (1995).
4. S. Kalkal *et al.*, Phys. Rev. C **81**, 044610 (2010).
5. H. Q. Zhang *et al.*, Phys. Rev. C **82**, 054609 (2010).
6. H.-J. Hennrich *et al.*, Phys. Lett. **B258**, 275 (1991).
7. A. M. Stefanini *et al.*, Phys. Rev. C **52**, R1727 (1995).
8. M. Trotta *et al.*, Phys. Rev. C **65**, 011601(R) (2001).
9. H. A. Aljuwair *et al.*, Phys. Rev. C **30**, 1223 (1984).
10. H. Timmers *et al.*, Nucl. Phys. **A633**, 421 (1998).
11. F. Scarlassara *et al.*, Nucl. Phys. **A672**, 99 (2000).
12. J. J. Kolata *et al.*, Phys. Rev. C **85**, 054603 (2012).
13. L. Corradi *et al.*, Nucl. Phys. **A685**, 37c (2001).
14. G. Pollarolo and A. Winther, Phys. Rev. C **62**, 054611 (2000).
15. M. Benjelloun *et al.*, Nucl. Phys. **A560**, 715 (1993).
16. P. Jacobs *et al.*, Phys. Lett. **B175**, 271 (1986).
17. A. M. Stefanini *et al.*, Nucl. Phys. **A456**, 509 (1986).
18. F. Scarlassara *et al.*, EPJ Web Conf. **17**, 05002 (2011).
19. F. L. H. Wolfs, Phys. Rev. C **36**, 1379 (1987).
20. K. T. Lesko *et al.*, Phys. Rev. C **34**, 2155 (1986).
21. Z. Kohley *et al.*, Phys. Rev. Lett. **107**, 202701 (2011).
22. E. Vulgaris *et al.*, Phys. Rev. C **33**, 2017 (1986).
23. K. Hagino, N. Rowley, and A. T. Kruppa, Comput. Phys. Commun. **123**, 143 (1999).
24. H. Q. Zhang *et al.*, Chin. Phys. C **34**, 1628 (2010).
25. A. Gavron, Phys. Rev. C **21**, 230 (1980).
26. Ö. Akyüz and A. Winther, in *Nuclear Structure and Heavy-Ion Reactions*, Proceedings of the International School of Physics "Enrico Fermi", Course LXXVII, Varenna, edited by R. A. Broglia *et al.* (North-Holland, Amsterdam, 1981).
27. E. F. Aguilera *et al.*, Phys. Rev. C **52**, 3103 (1995).x
28. K. Hagino *et al.*, Phys. Rev. Lett. **79**, 2014 (1997).
29. H. M. Jia *et al.*, Phys. Rev. C **86**, 044621 (2012).
30. S. L. Tabor *et al.*, Phys. Rev. C **17**, 2136 (1978).
31. R. Rascher *et al.*, Phys. Rev. C **20**, 1028 (1979).
32. Y. Eisen *et al.*, Nucl. Phys. **A291**, 459 (1977).
33. E. Bozek *et al.*, Nucl. Phys. **A451**, 171 (1986).
34. A. M. Borges *et al.*, Phys. Rev., C **46**, 2360 (1992).
35. C. P. Silva *et al.*, Phys. Rev. C **55**, 3155 (1997).
36. L. C. Chamon *et al.*, Phys. Lett. **B275**, 29 (1992).
37. M. Benjelloun *et al.*, Nucl. Phys. **A560**, 715 (1993).
38. P. Jacobs *et al.*, Phys. Lett. **B175**, 271 (1986).
39. R. F. Simões *et al.*, Phys. Lett. **B527**, 187 (2002).
40. P. D. Bond *et al.*, Phys. Rev. C **16**, 177 (1977).
41. Sunil Kalkal *et al.*, Phys. Rev. C **83**, 054607 (2011).